J Adv. Environ Health Res (2018) 6:173-178 DOI: 10.22102/JAEHR.2018.134412.1083

ORIGINAL PAPER

Hydrothermal synthesis and characterization of Tungsten-doped ZnO nanoparticles as an environmentally friendly substance

Yahya Zandsalimi[1], Behzad Shahmoradi [2], Saeed Dehestani Athar [2], Afshin Maleki [2,✉]

1. Student Research Committee, Kurdistan University of Medical Sciences, Sanandaj, Iran
2. Environmental Health Research Center, Research Institute for Health Development, Kurdistan University of Medical Sciences, Sanandaj, Iran

Date of submission: 02 Jul 2018, ***Date of acceptance:*** 01 Dec 2018

ABSTRACT

Hexagonal-structured zinc oxide (ZnO) is a semiconductor material with various industrial and cosmetic applications. Some of the main limitations of ZnO are aggregation, poor dispersibility, and wide energy gap, which limit its efficiency in some applications. The present study aimed to synthesize tungsten (W)-doped ZnO nanostructures using a hydrothermal method and characterize the particles to discover their application potency in various fields. To do so, 0.5%, 1.0%, and 2.0% of tungsten oxide (WO) were incorporated into the structure of ZnO, and the properties of the particles were determined via SEM, XRD, FTIR, AFM, DLS, and UV-Vis spectroscopy and zeta potential analysis. According to the obtained SEM images and XRD patterns, the prepared particles possessed hexagonal, non-aggregated structures. Furthermore, the UV-Vis spectra and AFM micrograms indicated that the doping of the ZnO nanostructures with tungsten caused a spectral shift in the absorbance of ZnO nanoparticles from the UV region to the visible light spectrum, increasing their relative roughness. According to DLS analysis, doping decreased the particle size of ZnO. In general, our findings demonstrated that the doping of ZnO nanostructures with tungsten could promote their efficiency and applicability in the treatment of environmental pollutants.

Keywords: Nanoparticle, Hydrothermal Synthesis, Zinc Oxide, Tungsten-Doped ZnO, Doping, Semiconductor

Introduction

Zinc oxide (ZnO) is a substance with unique properties, including the dual characteristics of semiconductor and piezoelectric materials. As a semiconductor, the exciton binding energy of ZnO is 60 meV, and its energy gap is 3.3 eV.[1] With such particular properties, ZnO has diverse applications. For instance, ZnO microparticles are used in burn ointments, antibacterial treatments, sunscreens, fabrication of transistors,[2] atomic force microscopy probes, screens, solar cell electrodes,[3] gas sensors,[4] rubber manufacturing, varistors and fire retardants, paints,[5] anticorrosion coatings, the glass industry, reduction of fusion points, and promoting chemical stability.[6]

In most of the applications, the efficiency of ZnO particles depends on their size and morphology, which could be controlled through synthesis. ZnO nanoparticles could be prepared through several synthesis approaches, including the sol-gel,[7] sonochemical,[8] microemulsion,[9] hydrothermal,[10] and chemical coprecipitation[11] methods. All the outlined methods have some limitations, such as inhomogeneous particle size distribution or the formation of large particles. To solve these issues, recent studies have recommended the coating of nanoparticles (NPs) to decrease their surface tension and agglomeration based on colloid chemistry. On the other hand, other researchers have suggested alternative synthesis methods.[12] Among various NP preparation routes, hydrothermal treatment is an appropriate option since it requires low operational pressure and temperature. In addition, it is an eco-friendly and non-hazardous approach, which

✉ *Afshin Maleki*
maleki43@yahoo.com

Citation: Zandsalimi Y, Shahmoradi B, Dehestani Athar S, Maleki A. Hydrothermal synthesis and characterization of Tungsten-doped ZnO nanoparticles as an environmentally friendly substance. J Adv Environ Health Res 2018; 6(3): 173-178

utilizes simple equipment without the need for post-treatment. In this method, particle sizes could be easily managed by maintaining the reaction temperature, process time, and concentration of the solution.[13]

In the case of ZnO NPs, the main limitations are the high energy gap, agglomeration, and poor particle dispersibility.[14] Researchers have attempted to overcome these issues by altering the structure of ZnO NPs using dopants or surface inhibitors. In fact, surface modification by surfactants has proven useful for avoiding aggregation, and doping is expected to decrease the energy gap and shift the required excitation wavelength from the UV range to the visible light spectrum.[15] Therefore, the doping of the structure of ZnO NPs using appropriate dopants is expected to improve their efficiency in the photodegradation of organic pollutants. The present study aimed to employ a hydrothermal method to synthesize tungsten (W)-doped ZnO NPs and assess the properties of the prepared particles.

Materials and Methods

Chemicals

This laboratory-scale, semi-empirical was conducted using various chemicals, such as ZnO, n-butylamine, NaOH (Merck, Germany), and tungsten oxide (WO) (Sigma Co.).

WO-ZnO Synthesis

The W-doped ZnO particles were synthesized using a hydrothermal method. Initially, 2 M ZnO and a definite molar percentage of WO (0.0%, 0.5%, 1.0% or 2.0%) were added to a Teflon lined stainless steel autoclave. Afterwards, 1 M NaOH (10 mL) and surfactant (0.5 mL) were combined with the ZnO and WO particles, and the autoclave was maintained for 12 hours at the temperature of 120 ºC. Following that, the autoclave contents were removed, washed with deionized water repeatedly, and dried in the air.[16]

Material Characterization

The dried product was subjected to characterization analysis, which consisted of powder X-ray diffraction (XRD) (Inel, EQUINOX 3000, France), scanning electron microscopy (SEM) (Tscan, MIRA3, Czech Republic), Fourier transform infrared spectra (FTIR) (Bruker-Tensor 27, Germany), atomic force microscopy (AFM) (Research Ara-Advance, Iran), and Zeta potential analyzers (Brookhaven- Nanobrook, USA) in order to determine the crystal structure, morphology, and surface chemistry, respectively.

Results and Discussion

SEM was used to determine the morphology and size of the ZnO particles, and the obtained SEM images are depicted in Figure 1. As can be seen, the hydrothermally prepared particles were completely distinctive and contained no agglomerated masses. Moreover, the doped particles had proper size distribution, the particle sizes were less than 100 nm, and the NPs had hexagonal morphologies.

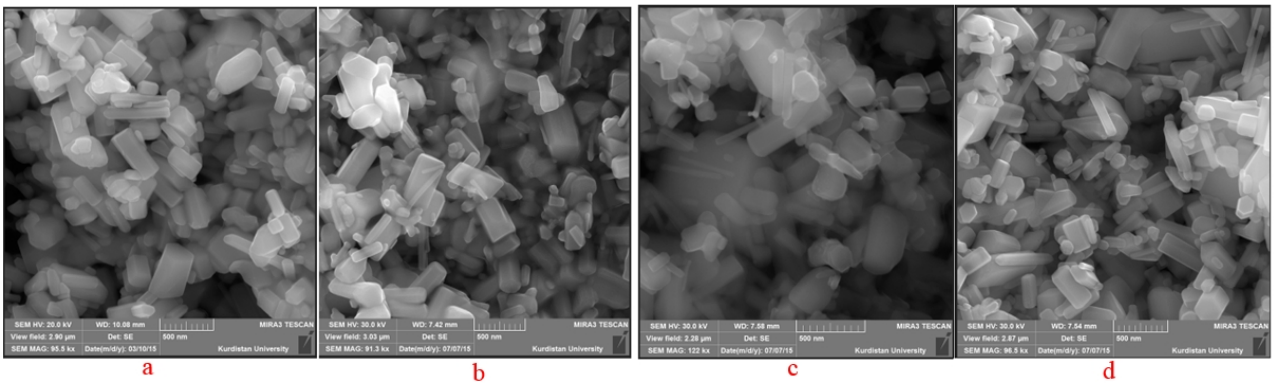

Fig. 1. SEM Images of nanoparticles a) ZnO b) WO-ZnO 0.5% c) WO-ZnO 1% d) WO-ZnO 2%

The un-doped and W-doped ZnO particles were investigated via XRD, and the obtained patterns are shown in Figure 2. The obtained XRD patterns exhibited three main peaks, which were associated with the (100), (002), and (101) ZnO crystal planes (JCPDC No. 36-1451). The lattice parameters of the un-doped samples were a=3.2491 and c=5.20710, while these values reduced in the doped samples. Furthermore, the density of the un-doped ZnO particles was estimated at 5.6470 g/cm^{-3}, which increased with the addition of the dopant.

Full width at half maximum (FWHM) is the simplest and most commonly applied method for the estimation of the average crystallite size, which is performed based on the diffraction peak using the Scherrer equation,[17] as follows:

$$\tau = \frac{K\lambda}{\beta \cos\theta} \quad (1)$$

where t is the average size of the Krystal (nm), K represents the crystal form factor, λ shows the wavelength of the manufacturer's x-ray tube (0.154 nm), and β is the peak width at the half maximum height. Calculation of the size of 2% W-ZnO using the Scherrer equation indicated that the size of the crystals was 64 nm.

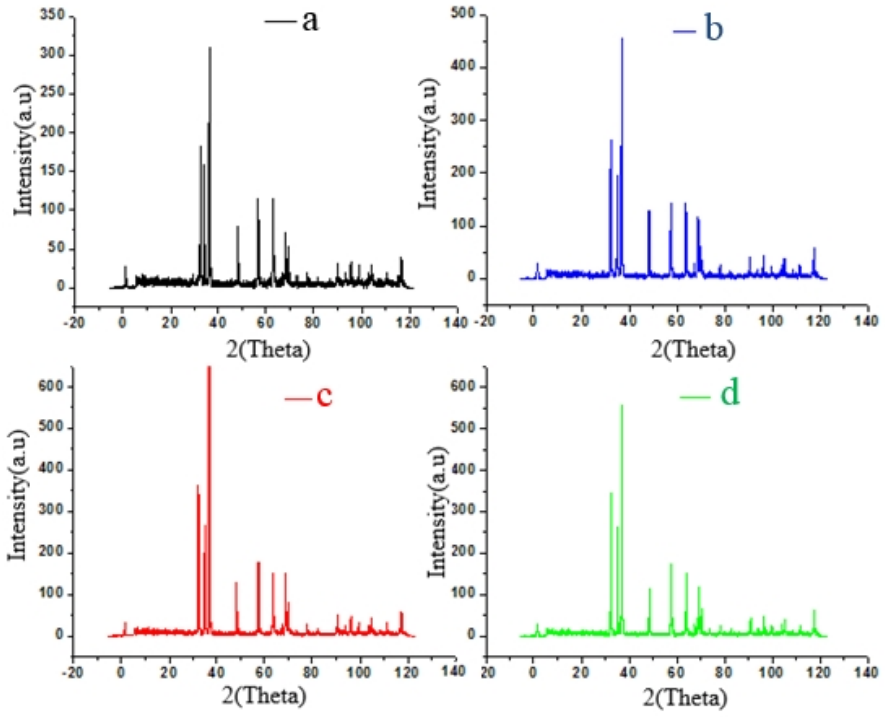

Fig. 2. XRD Diffractogram a) ZnO b) WO-ZnO 0.5% c) WO-ZnO 1% d) WO-ZnO 2%

The FTIR spectra of the samples are depicted in Figure 3. As can be seen, the spectra showed a strong vibrational band at 469 cm^{-1}, referring to the stretching vibration of Zn-O.[18]

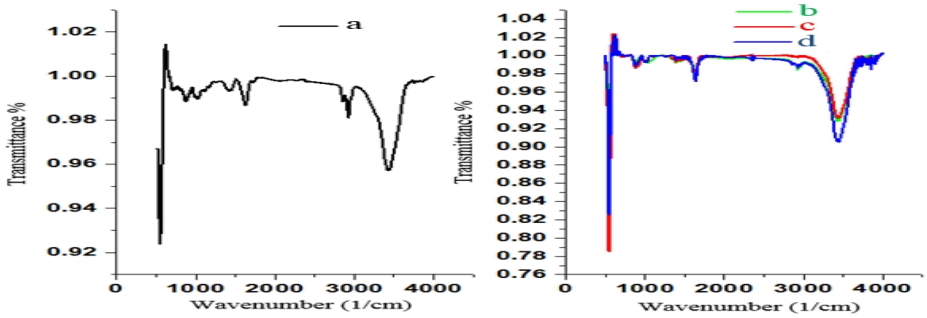

Fig. 3. FTIR Diffractogram a) ZnO b) WO-ZnO 0.5% c) WO-ZnO 1% d) WO-ZnO 2%

In addition to this peak, the spectra contained a peak at 1730 cm^{-1}, which could be ascribed to the C=O bond stretching of the carboxylic groups and a peak at 2918 cm^{-1}, which was indicative of the C-H bonds. In addition, the stretching vibrations of the N-H bonds of the amine groups appeared at 3448 cm^{-1} as the direct outcomes of adding the n-butylamine surfactant to the synthesis solution. Consistent with the present study, the findings of Mote have denoted the observation of the Zn-O stretching mode at 600-400 cm^{-1} and the N-H stretching vibration at 3600-3400 cm^{-1} in a study regarding Cr-doped ZnO NPs.[19]

To evaluate the effect of the dopant on the band gap energy of the ZnO NPs, the un-doped and W-doped samples were scanned using a UV-Vis spectrophotometer. The resultant spectra are illustrated in Figure 4. In line with the prior reports in this regard,[20] the absorbance peak of the un-doped ZnO samples was observed at 388 nm in the current research, which is within the UV range. However, the absorbance peaks of the doped samples shifted toward longer wavelengths and rose within the visible range of approximately 440 nm. In other words, the UV-Vis spectra had a peak shift from the UV light region to the visible spectrum. Since the doped samples could be excited by visible light, the W-doped ZnO NPs had the potential to be applied in visible light-driven processes. Such conclusion was also drawn in the study by Wang *et al*. in which ZnO was doped by nitrogen, and the authors declared that N-doping resulted in a shift in the absorbance peak of the un-doped ZnO from 384 to 450 nm.[21]

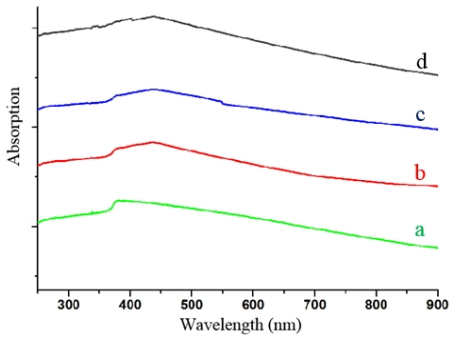

Fig. 4. Spectra of nanoparticles a) ZnO b) WO-ZnO 0.5% c) WO-ZnO 1% d) WO-ZnO 2%

Topography of the un-doped ZnO NPs and doped samples containing 2.0% WO was investigated by atomic force microscopy (AFM). According to the results of AFM (Figure 5), the relative roughness of the un-doped and W-doped ZnO particles was 3.291 and 1.7701, respectively. Therefore, W-doping could enhance the relative roughness of ZnO, thereby promoting dispersibility and pollutant adsorption capacity.

Particle Size Distribution

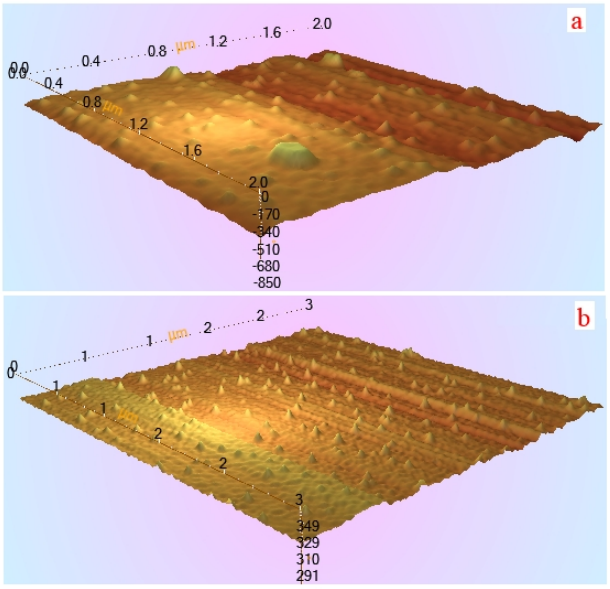

Fig. 5. AFM of nanoparticles a) ZnO b) WO-ZnO 2%

Since DLS analysis could measure the hydrodynamic particle size of the samples, which may be larger than the sizes determined by SEM, the samples were analyzed by DLS (Figure 6). As is evident, the W-doping of the ZnO particles reduced the particle size of ZnO and improved the distribution of the ZnO NPs. In this regard, the study by Shayesteh *et al*. entitled the "Effects of Doping and Annealing on the Physical Properties of ZnO:Mg Nanoparticles" indicated that the doping of ZnO with Mg reduced the size of the NPs. In addition, the effect intensified by increasing the Mg concentration, which could be due to the fact that Mg ions have a lower ionic radius compared to ZnO ions.[22]

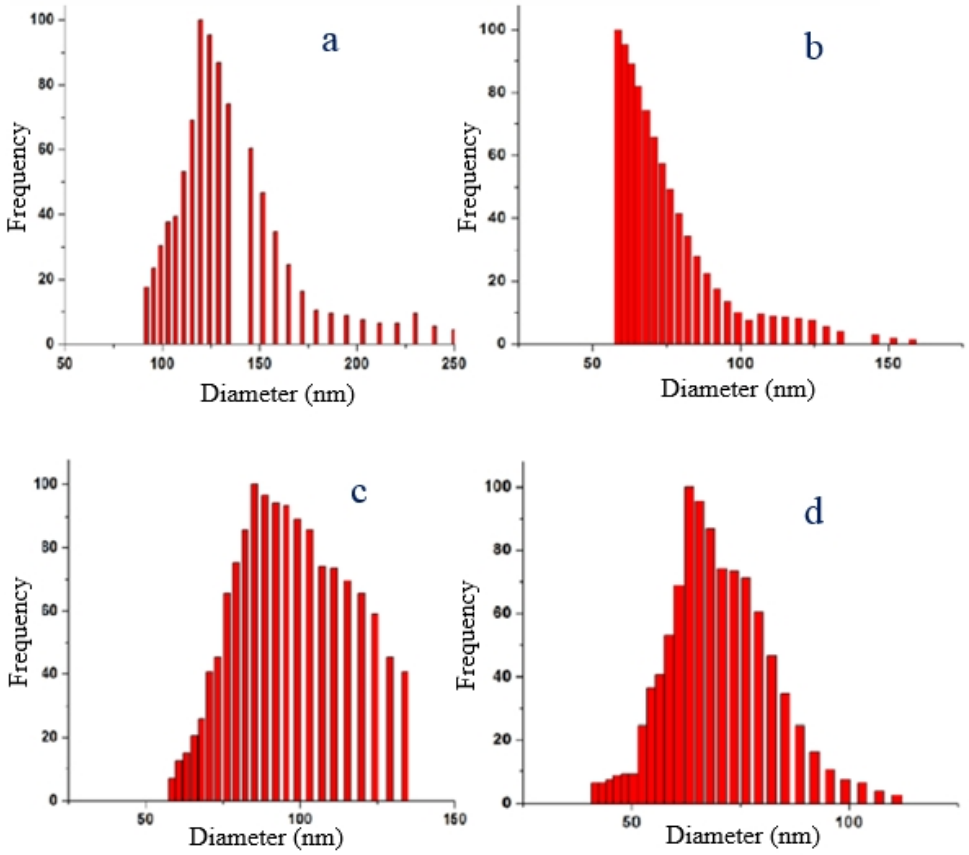

Fig. 6. DLS of nanoparticles a) ZnO b) WO-ZnO 0.5% c) WO-ZnO 1% d) WO-ZnO 2%

Zeta potential is essential to understanding and controlling the properties of colloidal suspensions. In the present study, the zeta potential of the pure ZnO doped with the molar percentages of 0.5, 1, and 2 tungsten oxide was measured at the optimal pH. To do so, a suspension of NPs (0.01 gram) was prepared in distilled water (5 ml), and all the samples were placed in ultrasonic instruments for 15 minutes before measuring the zeta potential. The zeta potential results are presented in Table 1. According to the information in the table, ZnO with tungsten NPs increased the zeta potential and movement, so that ZnO in the un-doped ZnO and WO-ZnO (2%) was -7.34 and -14.45 mV, respectively. Therefore, it could be concluded that doping increases the level and surface charge of ZnO NPs.

Table 1. Zeta potential of nanoparticles

Nanoparticles	Zeta Potential (mV)	Mobility (μ/s)/(V/cm)
WO-ZnO 0.5 %	- 11.65	- 0.91
WO-ZnO 1 %	- 14.88	- 1.16
WO-ZnO 2 %	- 14.45	- 1.13
undoped ZnO	- 7.34	- 0.57

Conclusion

According to the results, the SEM images of the synthesized NPs were hexagonal, which is consistent with ZnO. Furthermore, the hydrothermally synthesized NPs were completely distinctive and contained no agglomerated masses. The XRD analysis demonstrated three main peaks of (100), (002), and (101), which matched the crystalline structure of ZnO in the Moler index. The effect of the dopant on the energy band gap was also investigated. According to the results, the absorption of pure ZnO was 388 nm, while it was 440 nm in doped oxide. The results of AFM indicated that the relative roughness of the doped NPs increased compared to pure ZnO. Moreover, the DLS charts showed that doping reduced the size and uniformity of the ZnO particles. The zeta potential results demonstrated that doping could also increase the surface charge in ZnO NPs.

Acknowledgments

This article was extracted from a research dissertation conducted by the first author,

approved by the Environmental Health Research Center, and funded by Kurdistan University of Medical Sciences (IR.MUK.REC.1394.14516). Hereby, we extend our gratitude to the sponsors of the project.

References

1. He C, Sasaki T, Shimizu Y, Koshizaki N. Synthesis of ZnO nanoparticles using nanosecond pulsed laser ablation in aqueous media and their self-assembly towards spindle-like ZnO aggregates. App Surf Sci 2008; 254(7): 2196-2202.
2. Huang W-J, Fang G-C, Wang C-C. A nanometer-ZnO catalyst to enhance the ozonation of 2, 4, 6-trichlorophenol in water. Colloids Surf A Physicochem Eng Asp 2005; 260(1-3): 45-51.
3. Hamedani NF, Farzaneh F. Synthesis of ZnO nanocrystals with hexagonal (Wurtzite) structure in water using microwave irradiation. J Sci, Islam Republic Iran 2006; 17(3): 231-234.
4. Zhang Q, Xie C, Zhang S, Wang A, Zhu B, Wang L, et al. Identification and pattern recognition analysis of Chinese liquors by doped nano ZnO gas sensor array. Sens Actuators B Chem 2005; 110(2): 370-376.
5. Matsubara K, Fons P, Iwata K, Yamada A, Sakurai K, Tampo H, et al. ZnO transparent conducting films deposited by pulsed laser deposition for solar cell applications. Thin Solid Films 2003; 431: 369-372.
6. Lin H-M, Tzeng S-J, Hsiau P-J, Tsai W-L. Electrode effects on gas sensing properties of nanocrystalline zinc oxide. Nanostructured Mater 1998; 10(3): 465-477.
7. Livage J, Beteille F, Roux C, Chatry M, Davidson P. Sol–gel synthesis of oxide materials1. Acta Mater 1998; 46(3): 743-750.
8. Chuah G, Jaenicke S, Pong B. The preparation of high-surface-area zirconia: II. Influence of precipitating agent and digestion on the morphology and microstructure of hydrous zirconia. J Catal 1998; 175(1): 80-92.
9. López-Quintela MA, Tojo C, Blanco M, Rio LG, Leis J. Microemulsion dynamics and reactions in microemulsions. Curr Opin Colloid Interface Sci 2004; 9(3-4): 264-278.
10. Wang B, Callahan M, Xu C, Bouthillette L, Giles N, Bliss D. Hydrothermal growth and characterization of indium-doped-conducting ZnO crystals. J Cryst Growth 2007; 304(1): 73-79.
11. Heitjans P, Indris S. Diffusion and ionic conduction in nanocrystalline ceramics. J Phys Condens Matter 2003; 15(30): R1257.
12. Liang Y-Y, Zhang L-M, Li W, Chen R-F. Polysaccharide-modified iron oxide nanoparticles as an effective magnetic affinity adsorbent for bovine serum albumin. Colloid Polym Sci 2007; 285(11): 1193-1199.
13. Farhat I, El-Hawary M. Optimization methods applied for solving the short-term hydrothermal coordination problem. Elect Power Sys Res 2009; 79(9): 1308-1320.
14. Shahmoradi B, Ibrahim I, Namratha K, Sakamoto N, Ananda S, Somashekar R, et al. Surface modification of indium doped ZnO hybrid nanoparticles with n-butylamine. Int J Chem Eng Res 2010; 2(2): 107-117.
15. Dresselhaus MS, Dresselhaus G, Saito R, Jorio A. Raman spectroscopy of carbon nanotubes. Phy Rep 2005; 409(2): 47-99.
16. Shahmoradi B, Namratha K, Byrappa K, Soga K, Ananda S, Somashekar R. Enhancement of the photocatalytic activity of modified ZnO nanoparticles with manganese additive. Res Chem Intermediat 2011; 37(2-5): 329-340.
17. Zimmer C, Wright Jr S, Engelhardt R, Johnson G, Kramm C, Breakefield X, et al. Tumor cell endocytosis imaging facilitates delineation of the glioma–brain interface. Exp Neurol 1997; 143(1): 61-69.
18. Jae KY, Hun KK, Sung LC, Bo SK. Characterization of ZnO nanopowders synthesized by the polymerized complex method via an organochemical route. Journal of Ceramic Processing Research 2002.
19. Mote VD, Huse VR, Dole BN. Synthesis and characterization of Cr doped ZnO nanocrystals. World J Condens Matt Phy 2012; 2(04): 208.
20. Kumbhakar P, Singh D, Tiwary C, Mitra A. Chemical synthesis and visible photoluminescence emission from monodispersed ZnO nanoparticles. Chalcog Lett 2008; 5(12): 387-394.
21. Wang Y, Lau S, Zhang X, Lee H, Hng H, Tay B. Observations of nitrogen-related photoluminescence bands from nitrogen-doped ZnO films. J Cryst Growth 2003; 252(1-3): 265-269.
22. Shayesteh SF, Dizgah AA. Effect of doping and annealing on the physical properties of ZnO: Mg nanoparticles. Pramana 2013; 81(2): 319-330.